# Further Information from a Sonometric Study of the Normal Tricuspid Valve Annulus in Sheep: Geometric Changes during the Cardiac Cycle

Jerome Jouan, Matthew R. Pagel, Matthew E. Hiro, Khee Hiang Lim, Emmanuel Lansac, Carlos M. G. Duran

*The International Heart Institute of Montana Foundation at St. Patrick Hospital and Health Sciences Center and The University of Montana, Missoula, Montana, USA*

***Background and aim of the study:*** **In a previous sonometric study, changes were described that occurred in the normal tricuspid valve during the cardiac cycle. However, the wealth of data available suggested the need for reporting further findings that should contribute to a better understanding of the dynamics of the tricuspid valve.**
***Methods:*** **Thirteen sonomicrometry transducers were placed in the hearts of each of seven sheep. Six transducers were placed in the tricuspid annulus (TA), at the base of each leaflet, and at each commissure; three at the tips of the papillary muscles (PMs); three in the free edges of the leaflets; and one transducer was placed at the apex. Distances between transducers, pulmonary and right ventricular pressures, and pulmonary flow were recorded simultaneously.**
***Results:*** **The TA area underwent two major contractions and expansions during the cardiac cycle, reaching its maximum during isovolumic relaxation and its minimum in diastole. The TA height-to-width ratio changed from 8.4 ± 1.9% to 15.3 ± 4.2%. The leaflets began to open before end-systole. By the end of isovolumic relaxation, the leaflets had completed 54.1 ± 13.4% of their opening. The PM and TA planes were not parallel, but were offset by 11.5 ± 1.9° to 17.8 ± 2.1°. The PM rotated 6.9 ± 0.9° with respect to the TA, with 3.1 ± 1.1° of the rotation occurring during ejection.**
***Conclusion:*** **The tricuspid valve is not a passive structure but rather forms a dynamic part of the right ventricle. Its orifice area changes not only due to the contraction and expansion of its perimeter but also to changes in its saddle shape. Leaflet opening and closure is not simply a response to pressure. The PMs rotate in relation to the TA. These data should impact upon the diagnosis and surgery of functional tricuspid regurgitation.**

The Journal of Heart Valve Disease 2007;16:511-518

There is a paucity of information available on the functional anatomy of the tricuspid valve when compared with other cardiac valves. In an attempt to analyze the geometric changes of the tricuspid valve during the cardiac cycle, previous experience with sonomicrometry in studies of the aortic (1,2) and mitral valves (3) was applied. Although the preliminary results of the present study were reported previously (4), the wealth of data available suggested a need to publish further findings that contribute to a better understanding of the dynamics of the tricuspid valve.

Address for correspondence:
Prof. Carlos M. G. Duran MD, PhD, The International Heart Institute of Montana Foundation, 500 West Broadway, Suite 350, Missoula, MT 59802, USA
e-mail: duran@montana.com

## Materials and methods

### Experimental design

Seven adult Targhee sheep (bodyweight 69 ± 9 kg) underwent implantation of 13 sonomicrometry transducers on the tricuspid valve using cardiopulmonary bypass (CPB); the mean pump time was 135 ± 4 min, and cross-clamp time 88 ± 2 min.

The surgical techniques used have been reported previously (4). In brief, while the animal was under general anesthesia, the heart was approached through a right lateral thoracotomy, and the sheep was placed on normothermic CPB with bicaval and aortic cannulations. The aorta was cross-clamped, and antegrade cold crystalloid cardioplegia employed.

In order to study the tricuspid valve complex, 13 transducers (Sonometrics Corporation, London, Ontario, Canada) were implanted. To avoid inter-operator variability, all transducers were placed by the same surgeon. Ten 2-mm ultrasonic transducers were

J Heart Valve Dis
Vol. 16. No. 5
September 2007

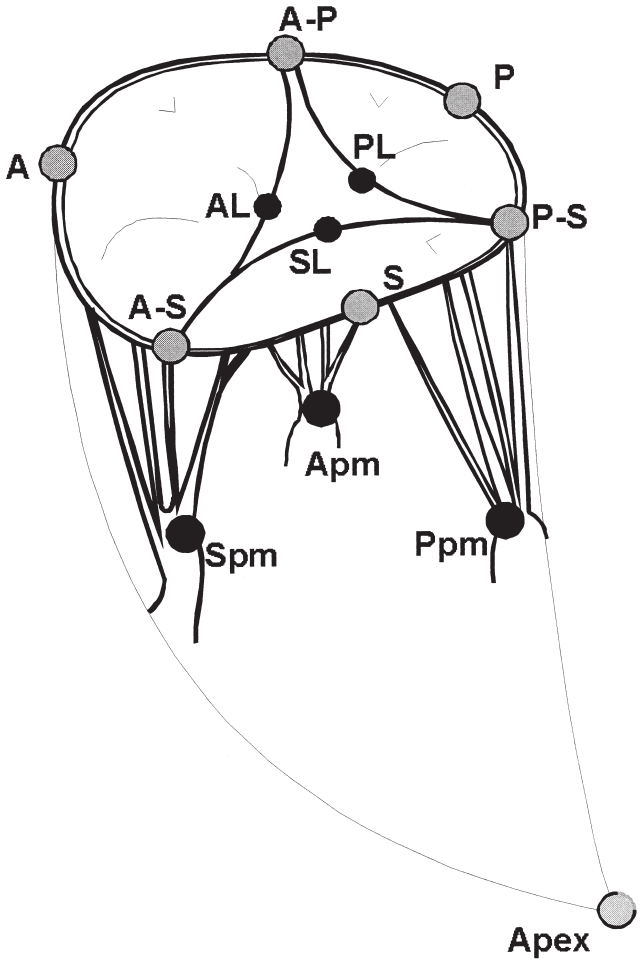


*Figure 1: Location of the 13 transducers placed in the tricuspid valve at the apex of the left ventricle (Apex); the midpoint of the bases of the anterior (A), posterior (P), and septal (S) leaflets; the free edges of the anterior (AL), posterior (PL), and septal (SL) leaflets; the anteroposterior (A-P), anteroseptal (A-S), and posteroseptal (P-S) commissures; and the anterior (Apm), posterior (Ppm), and septal (Spm) papillary muscles.*

sutured along the tricuspid annulus (TA) (n = 6) at the anteroseptal, anteroposterior, and posteroseptal commissures, and at the relative midpoint of the base of the septal, anterior, and posterior leaflets (Fig. 1). Transducers were also placed inside the right ventricle (n = 3) at the tips of the septal, anterior, and posterior papillary muscles (PMs). Smaller, 0.7-mm transducers (n = 3) were sutured to the free edge of the septal, anterior, and posterior leaflets. The electrodes of the transducers on the TA and leaflets were exteriorized through the right atriotomy, and the electrodes of the transducers on the PMs were exteriorized through the right ventricular wall. One transducer was sutured to the apex of the heart as a reference transducer. High-fidelity, catheter-tipped pressure transducers (Model 510; Millar Instruments, Houston, TX, USA) were placed within the lumen of the pulmonary artery and in the right ventricle. A flowmeter ring (Transonic Systems Inc., Ithaca, NY, USA) was placed around the pulmonary trunk.

After discontinuing CPB, and when the animal was hemodynamically stable (≥15 min), the transducer distances were recorded along with right ventricular pressure, pulmonary trunk pressure, and pulmonary artery flow. All recordings were performed at 200 Hz. Epicardial, two-dimensional echocardiography with color Doppler was used to assess the competence and anatomy of the tricuspid valve before and after implantation of the transducers. On completion of the experiment the heart was arrested by a lethal injection of potassium chloride, and the correct positions of the transducers verified.

All animals received humane care in compliance with the principles of the Animal Welfare Act, the *Guide for Care and Use of Laboratory Animals* from the United States Department of Agriculture, and the Institutional Animal Care and Use Committee of The University of Montana.

**Data acquisition and processing**

A postprocessing program (Sonometrics Corporation, London, Ontario, Canada) was used to examine each distance measurement between transducers. All distances and pressures were synchronized with the electrocardiogram and recorded at the same time with the Sonometrics system. Another postprocessing program (SonoXYZ; Sonometrics Corporation) was then used to generate distance measurements between all transducers.

The distances were used to create a three-dimensional (3-D) coordinate system based on the least-squares plane of the TA using MATLAB software (The Math Works, Inc., Natick, MA, USA). The distances were first used to define an arbitrarily placed Cartesian coordinate system. The coordinate system was then shifted to the TA to establish a meaningful reference frame, as described previously by Gorman et al. (5). The centroid of the TA transducers was calculated and set as the origin of this system. The approximate plane of the TA was determined by least-squares regression of the TA transducer coordinates and set as the x-y plane. The positive z axis was aligned normal to the least-squares plane opposite to the direction of blood flow. The x-z plane was directed through the posteroseptal transducer. The x-z plane and the least-squares x-y plane thus defined the x axis. Finally, the y axis was chosen orthogonal to positive x and positive z in a right-handed coordinate system. The resulting system represented an approximation of the apicobasal direction (z axis), the anterior-posterior direction (x axis), and the medial-lateral direction (y axis).

*Table I: Percentage changes in tricuspid orifice area (% open) during the phases of the cardiac cycle.*

| | ED | IVC | ES | IVR | Max. | Min. |
|---|---|---|---|---|---|---|
| Orifice area (% open) | 63.6 ± 9.6 | 27.4 ± 8.2 | 14.1 ± 4.2 | 54.1 ± 13.4 | 100 | 0 |

ED: End-diastole; ES: End-systole; IVC: Isovolumic contraction; IVR: Isovolumic relaxation.

**Analysis of tricuspid geometry**

The coordinates of the transducers formed a 3-D skeleton of the tricuspid valve, which allowed for the precise measurement of specific anatomic features and an approximation of the entire valve geometry.

The TA area, measured by the addition of six triangles (each containing two contiguous TA transducers projected into the least-squares plane and the centroid), was calculated using the Heron formula (6,7).

A variation of the method of Salgo et al. (8) was used to define the saddle shape of the mitral valve annulus as the ratio between annulus height and commissural width: annulus height-to-width ratio (AHWR). For this study of the tricuspid valve, the ratio was calculated as the ratio of annular maximum height (the dimension normal to the least-squares plane of the TA) to the maximum in-plane dimension. The relationship between AHWR and TA area was investigated by Fourier analysis (9). The correlation between changes in AHWR and TA area at the three frequencies of most significant change was then calculated. The resulting correlation coefficients related changes in AHWR to TA area.

The tricuspid orifice area, defined as the triangular area formed by the leaflet tips, was used to determine the opening and closing of the valve. The valve was defined as being 0% open at minimum orifice area, and 100% open at maximum orifice area; intermediate values were calculated on a linear scale.

Angles of PM excursion were calculated between the least-squares plane and a vector from the PM transducer to the corresponding annular commissure. Rotation of the three lines forming the PM triangle was measured relative to their position at end-diastole, and the average of the three measurements was calculated to measure PM rotation. Counter-clockwise rotation with respect to the TA, as viewed from the heart base, was defined as positive.

Geometric changes were time-related to each phase of the cardiac cycle using pulmonic and right ventricular pressure curves. End-diastole, or the beginning of systole, was defined as the point of increasing right ventricular pressure tracing ($dP/dt > 0$). The end of isovolumic contraction (IVC) was defined as the beginning of ejection at the crossing point of the right ventricular and pulmonic pressure curves. The dicrotic notch in the pulmonic pressure curve defined the end of systole. The end of isovolumic relaxation (IVR) was defined as the lowest point of the right ventricular pressure tracing after ejection ($dP/dt = 0$) (10). The ventricular ejection and filling periods were then split in half (S1 and S2; D1 and D2, respectively).

After close examination of the data, three consecutive heartbeats with the least amount of noise were chosen for analysis. Summary statistics were reported as mean ± SEM. Changes in distance were tested by conducting the two-tailed *t*-test for paired comparisons with a significance level of $p \leq 0.05$. All statistical analyses were performed using Excel (Microsoft Corporation, Seattle, WA, USA) and MATLAB.

## Results

**Model characteristics**

At the time of recording, the hemodynamic conditions were: heart rate 99 ± 6 beats/min; arterial pressure 67/40 ± 2/3 mmHg; stroke volume 33 ± 2 ml; and cardiac output 2.9 ± 0.4 l/min. The valves were shown to be competent on epicardial echocardiography in all animals. At necropsy, all transducers were in the correct positions in six animals. In one sheep, two PM transducers were incorrectly placed. All calculations which were dependent on the correct positioning of these two transducers were excluded.

**Tricuspid annulus changes**

The TA orifice area expands and contracts twice during the cardiac cycle (see Table I). During IVC and at the beginning of ejection, the TA contracts 18 ± 8% of the total change in TA area, reaching a minimum area of 480 ± 80 $mm^2$ (Figs. 2 and 3). During the rest of the ejection and the first half of IVR, the TA underwent major expansion (46 ± 12% of its total relaxation), reaching a maximum area of 610 ± 90 $mm^2$. During the second half of IVR, a second TA contraction occurred (27 ± 7% of the total change in area). The latter contraction continued during D1, and was followed by re-expansion during D2.

The reduction in the TA area was due in part to contraction of its perimeter, as reported previously (4). However, this total contraction of 7.9 ± 1.0% was not homogeneous. The septal contraction was slightly smaller than that of the anterior or posterior segments,

J Heart Valve Dis
Vol. 16. No. 5
September 2007

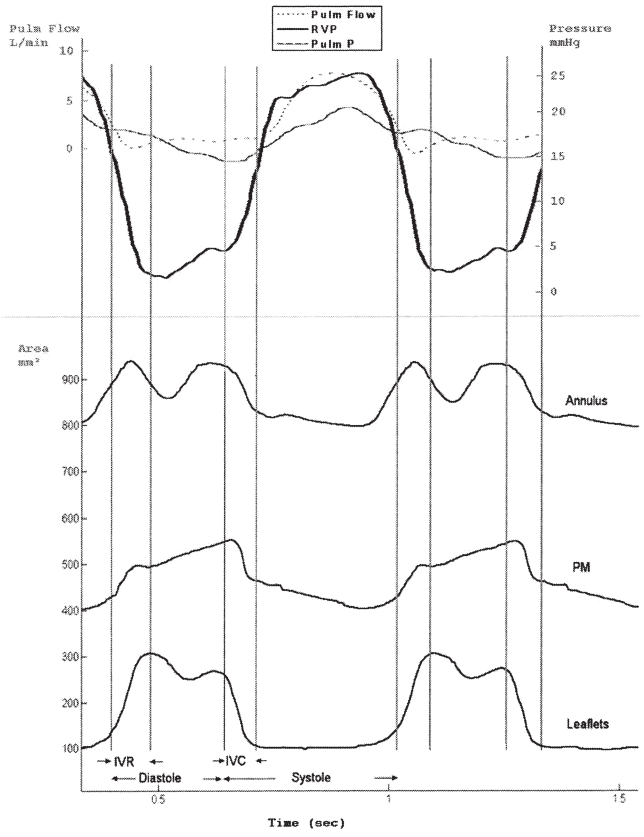


*Figure 2: Top: Pressure curves of blood flow in the pulmonary artery (Pulm Flow), the right ventricle (RVP), and the pulmonary artery (Pulm P). Bottom: Changes in the areas delineated by the ultrasound transducers placed around the tricuspid annulus (Annulus), the tips of the three papillary muscles (PM), and the free edges of the three leaflets (Leaflets) during two cardiac cycles. These recordings allowed the cardiac cycle to be split into diastole, systole, isovolumic contraction (IVC), and isovolumic relaxation (IVR).*

but not statistically significant (p = 0.254 and p = 0.089, respectively).

Perimeter contraction alone does not explain the reduction in TA area. The minimum diameter of the TA (approximately perpendicular to the septum) contract-

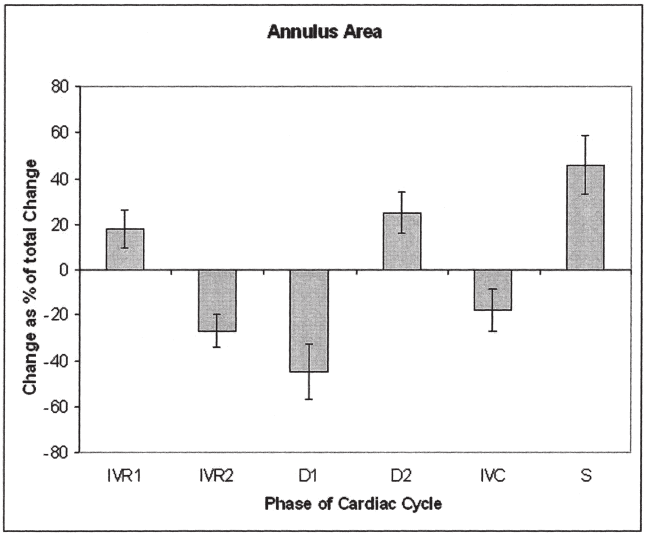


*Figure 3: Changes in tricuspid annulus area during the phases of the cardiac cycle as a percentage of the total change from minimum to maximum. IVR1: First half of the isovolumic relaxation phase; IVR2: second half of isovolumic relaxation phase; D1: first half of diastole; D2: second half of diastole; IVC: isovolumic contraction phase; S: systole.*

ed by 16.8 ± 1.5% (from 21.2 ± 2.0 mm to 17.8 ± 1.9 mm). This reduction of 9.3 ± 0.8% was greater than the contraction of the maximum diameter (roughly parallel with the septum), from 40.1 ± 2.6 mm to 36.4 ± 2.4 mm ($p < 0.0001$). This change in minimum diameter has a strong linear relationship with the TA area ($r = 0.88 \pm 0.08$), because the orifice becomes more ellipsoid (area = $\pi/4 \times$ minor diameter $\times$ major diameter).

Vertical displacement of the transducers placed around the TA was also observed throughout the cardiac cycle (Figs. 4b and c). When the TA contracted, its AHWR was changed from a minimum of 8.4 ± 1.9 to a maximum of 15.3 ± 4.2 (median ± SEM; here, the median was used rather than the mean to mitigate the effect of possible outliers). This change in AHWR was due to a 69.5 ± 10.5% increase in annular height ($r = 0.97 \pm 0.01$ for the correlation between AHWR and annular height).

*Table II: Changes during the phases of the cardiac cycle in the angles formed by vector of papillary muscle (PM) tips to corresponding commissure and the annulus plane.*

| PM region | D2 | IVC | S1 | S2 | IVR | D1 | Min. | Max. |
|---|---|---|---|---|---|---|---|---|
| Septal | 84.9 ± 10.1 | 83.4 ± 9.2 | 87.7 ± 9.8 | 89.8 ± 9.6 | 87.6 ± 11.2 | 87.0 ± 11.0 | 81.7 ± 9.7 | 91.8 ± 10.3 |
| Anterior | 95.0 ± 8.8 | 92.3 ± 9.6 | 79.4 ± 8.4 | 76.8 ± 7.4 | 86.4 ± 10.0 | 93.0 ± 9.6 | 74.6 ± 7.4 | 96.3 ± 9.1 |
| Posterior | 89.0 ± 7.6 | 88.4 ± 6.9 | 87.8 ± 5.9 | 85.2 ± 5.8 | 86.0 ± 5.8 | 87.5 ± 7.7 | 83.2 ± 6.2 | 92.3 ± 6.8 |

D1: First half of diastole; D2: Second half of diastole; IVC: Isovolumic contraction; IVR: Isovolumic relaxation; S1: First half of systole; S2: Second half of systole.

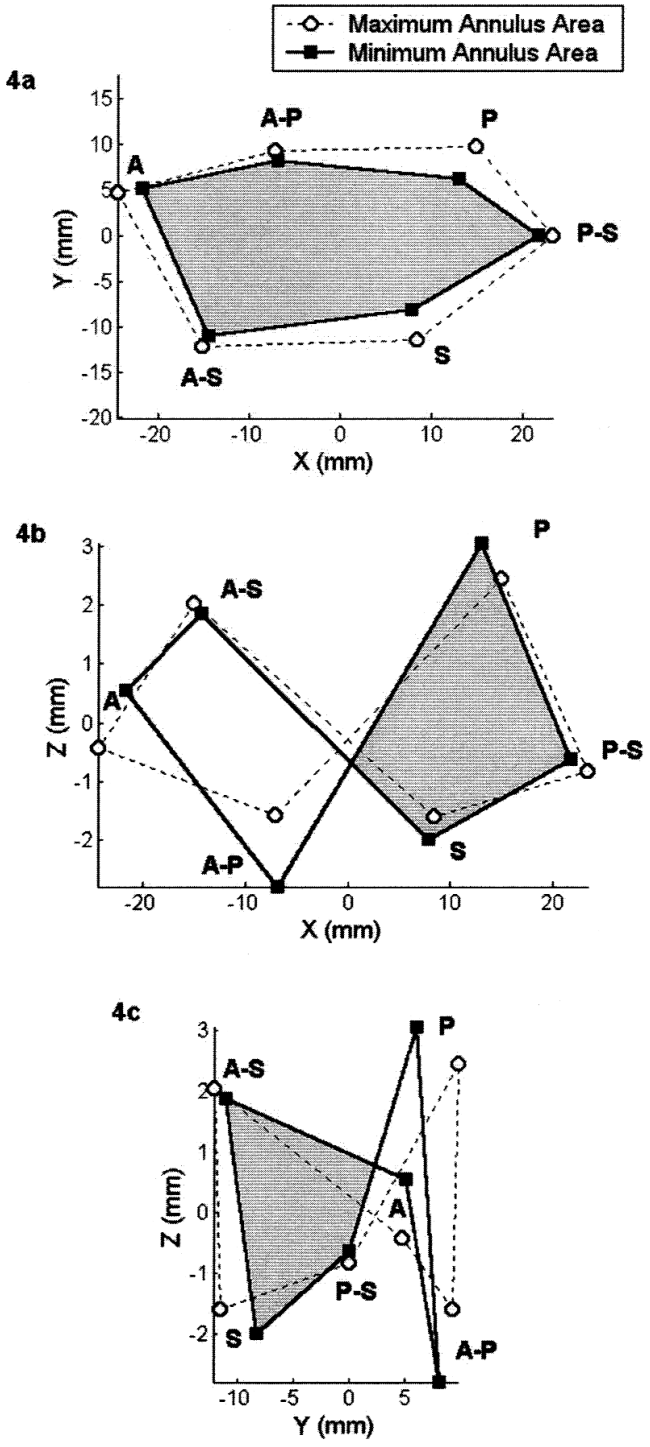


*Figure 4: Orthogonal representations of the tricuspid annulus at maximum (dotted line) and minimum (continuous line) area during the cardiac cycle. Circles and squares represent the location of transducers at the midpoint of the bases of the anterior (A), posterior (P), and septal (S) leaflets, and at the anteroposterior (A-P), anteroseptal (A-S), and posteroseptal (P-S) commissures. Two relative maxima can be noted in the x-z (4b) and y-z (4c) planes. P and A-S represent the pommel and the cantle of the tricuspid valve's saddle shape. The representation of the x-y plane is shown in Fig. 4a.*

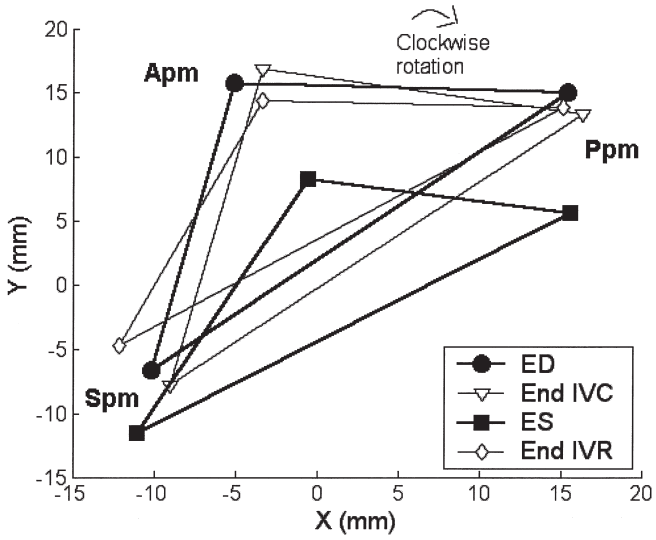


*Figure 5: Projection of papillary muscle rotation in the x-y plane. Three lines connect the anterior (Apm), posterior (Ppm), and septal (Spm) papillary muscles to form a triangle. Each triangle shows a different phase of the cardiac cycle: end of diastole (ED), end of isovolumic contraction (End IVC), end of systole (ES), and end of isovolumic relaxation (End IVR). Rotation is clockwise as seen from the base of the heart (arrow).*

**Leaflet motion**

Figure 2 shows that the leaflets began to open near the end of systole, completing 54.1 ± 13.4% of their opening by the end of IVR; however, in three sheep, opening was complete at that point (Fig. 2 represents one of these animals). The second peak in opening occurred near end-diastole, followed by closure during IVC.

**Papillary muscle movement**

The motion of the PMs relative to the TA plane can be described as a combination of shifting, bending, and twisting of the right ventricle. During the cardiac cycle, the centroid of the three PMs moved by 4.9 ± 1.3 mm in the y-direction, approximately perpendicular to the septum, and only 1.8 ± 0.7 mm in the x-direction, roughly parallel to the septum. In systole, the centroid moved 4.1 ± 1.1 mm towards the septum.

Angular displacements of the PMs below the corresponding commissures are summarized in Table II, and showed that, during IVR and D1, the septal PM moved toward the lateral wall by 19.0° and 16.9°, respectively. Simultaneously, the anterior PM moved by 30.3° and 29.5° in the same direction.

While all PM tips had a similar displacement in the z-direction (septal 3.0 ± 0.5 mm; anterior 2.8 ± 0.4 mm; posterior 2.4 ± 0.7 mm), the PM centroid moved only 1.4 ± 0.5 mm. Therefore, the PM plane is not parallel to

J Heart Valve Dis
Vol. 16. No. 5
September 2007

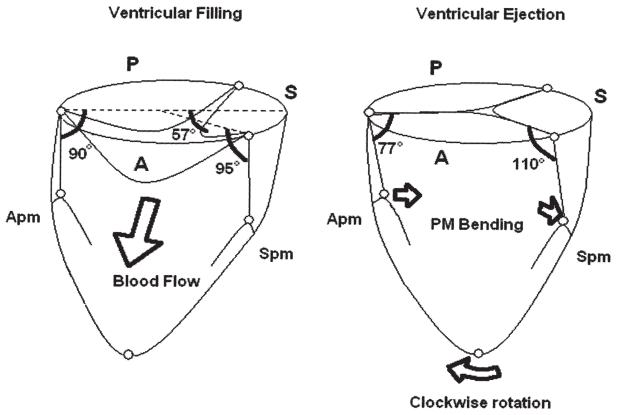


*Figure 6: Schematic representation of the lateral bending and rotation of the right ventricle extrapolated from angular values of the anterior (Apm) and septal (Spm) papillary muscles in respect to the tricuspid annulus (for one sheep). Open circles represent the location of commissural transducers between the anterior (A), posterior (P), and septal (S) leaflets. During ventricular filling, the anterior and posterior papillary muscles move outward, and the opening angle of the septal leaflet is limited to less than 60°, directing blood flow towards the lateral wall.*

the TA plane, and the PMs do not move together in the z-direction. In fact, the angle between the two planes changed by 6.4 ± 1.5°, from 11.5 ± 1.9° in diastole to 17.8 ± 2.1° in systole.

The maximum rotation of the PMs from end-diastole was 2.1 ± 1.0°, and the minimum value was -4.9 ± 1.1°, with a range of 6.9 ± 0.9°. The rotation at the end of IVC (0.5 ± 0.6°) was practically the limit of the systolic counter-clockwise rotation (as seen from the base of the heart). From IVC to end of systole, the PMs rotated clockwise by 3.3 ± 1.1° (Fig. 5).

## Discussion

Previously, the diagnostic and surgical methods for treating functional tricuspid regurgitation have very closely followed those applied to the mitral valve. However, the tricuspid valve has distinguishing characteristics that are often ignored. Its tendency to vary in degree following hemodynamic changes makes its evaluation difficult and unreliable. Because its pathology has also been considered secondary to left-sided lesions and pulmonary hypertension, tricuspid disease has been assumed spontaneously to revert after these lesions had been treated. These factors, together with its characteristic paucity of clinical manifestations, have resulted in a lack of solid principles for its diagnosis, indications, and appropriate surgical maneuvers. Advances in echocardiography and its increasing use in heart-failure patients have revealed a high prevalence of functional tricuspid regurgitation. Indeed, an awareness of its importance has led to a critical analysis of the results of tricuspid annuloplasty. A recent review of 790 patients who underwent a variety of tricuspid annuloplasties showed that between 15% and 37% of these cases had recurrent severe regurgitation at eight years' follow up (11). These results suggest that present annuloplasty techniques are either unreliable or insufficient. A deeper knowledge of the continuous changes in the shape of the tricuspid valve should aid in both understanding the mechanisms of its dysfunction and in developing new interventional therapies.

Previous experimental and clinical studies have shown that the TA continuously changes size and shape (4,12,13). In the present study, although the TA area contracted to 22% of its maximum area, the maximum reduction of the TA perimeter was only 7.9 ± 1.0%. The change in TA shape appears to be the main method of orifice reduction. An earlier report (4) showed that the ratio of the minimum-to-maximum diameters changed from 0.55 ± 0.05 to 0.46 ± 0.04 as the TA became less circular. In the present study, a high linear correlation was found between TA area and minimum TA diameter, with a displacement of the anteroposterior commissure toward the septum, resulting in a more elliptical TA. This change in shape is the main mechanism responsible for the TA area reduction, and questions the efficiency of rigid annuloplasty devices that interfere with this mechanism. This feature, which also was observed by Tsakiris et al. (12) using biplane angiography, has been attributed in recent magnetic resonance imaging (MRI) studies to septum thickening and twisting (14,15). The present model does not allow any description to be made of the absolute movements of transducers, and therefore these observations cannot be confirmed.

The perimeter contraction is consistent with the observed 15% shortening of the heart's sarcomeres (16) if it is postulated that both the anterior and posterior segments, as a part of the right ventricle free wall, are made from the transverse-oriented muscle fibers described macroscopically by Torrent-Guasp et al. (17) and histologically by Greenbaum et al. (18). As in the anterior segment of the mitral valve's annulus (which has been shown to change in health and disease (19,20)), the length of the tricuspid valve's septal segment also changes significantly during the cardiac cycle. This finding challenges both the standard method of using the length of the septal leaflet base to select the correct ring size as well as the use of open annuloplasty bands, which may not prevent further dilatation of the diseased TA.

The biphasic nature of the TA area curve is comparable to that observed in the mitral valve by Gorman et

al. (21), and in the tricuspid valve by Tei et al. (13) and Tamiya et al. (22). The maximum TA area occurred during IVR. This has not been reported previously, and is most likely due to relaxation of the right ventricular transverse fibers in late systole (23). TA contraction begins during IVR and continues through the first half of diastole; this period is not well understood, but it may help to empty the right atrium.

Starting with the beginning of IVC, a second contraction occurs, which reduces the TA to its minimum area for the entire cardiac cycle. This TA contraction corresponds to closure of the valve completed at the end of IVC.

Changes in the saddle shape of the TA also contribute to its orifice area. The increase in AHWR - that is, the increase in the saddle shape during contraction - has a 'folding', reducing effect on the TA. The high and low points of the saddle move away from each other in the apical/basal direction during TA area contraction. The saddle shape of the mitral valve annulus has been shown to minimize leaflet stress (8); it also allows a 'folding' of the annulus that effectively reduces its orifice area without a dramatic reduction in perimeter. Again, this annulus-reducing mechanism is compromised when a rigid, mono-planar annuloplasty ring is implanted.

The tricuspid leaflets start to open at the beginning of IVR, and reach maximum opening at the end of IVR. This finding raises questions about the mechanism of valve opening. Because the right ventricular pressure is greater than the right atrial pressure until the end of IVR, a pressure gradient cannot be the only mechanism for valve opening; indeed, TA contraction and PM motion may pull the leaflets open. Previously (4), it was shown that the TA had completed more than half of its contraction by the time of maximum leaflet excursion.

Higashidate et al. (24) reported that the two peaks of maximum orifice area corresponded to rapid ventricular filling and atrial kick, suggesting that valve closure could not occur before the beginning of ventricular systole. The results of the present study confirm these data, and show that complete valve closure occurs only at the end of IVC, providing further evidence that leaflet motion is not simply a result of the pressure gradient.

The chordae which anchor the septal leaflet to both PMs have been shown to be shorter in the tricuspid valve (25). Thus, the observed rightward displacement of the septal PM and posterior PM during the first part of ventricular filling is consistent with the restrictive pattern of septal leaflet opening reported earlier (4). Moreover, the anterior PM moved simultaneously in the same direction, which may indicate that blood flow is directed preferentially from the right atrium to the lateral part of the right ventricle. The pattern is reversed during ejection, and both PMs are displaced toward the left ventricle, aligning the flow toward the right outflow tract (Fig. 6).

Studies with tagged MRI (26) and tantalum markers (27) have described the main systolic pattern of rotation of the left ventricle; however, little is known about the twisting motion of the right ventricle. The clockwise rotation of the PMs (representing the apical loop of the right ventricle) relative to the TA (representing the basal right ventricle) is evidence of the twisting of the entire right ventricle. However, further non-invasive MRI studies are required to confirm this finding.

**Study limitations**

All data were acquired in an acute, anesthetized, open-chest, open-pericardium animal model. The deleterious effect of CPB and ischemia might have resulted in abnormal valve and ventricular behavior. The high heart rate and depressed diastolic arterial blood pressure as compared to pre-CPB measurements might have altered tricuspid motion during the cardiac cycle. The pericardium was not closed during measurements, eliminating its restraining effect on the right ventricle. The pre- and after-load conditions at the time of data recording were not controlled, and most likely varied extensively between animals. However, findings on the changes in TA area and leaflet opening motion were very similar to those reported previously.

Right ventricular motion analysis was deducted from the lateral and angular displacements of the transducers placed on the tip of each PM. Although these displacements should not be affected by contraction of the PM (which mainly occurs parallel to the long axis of the heart), further myocardial studies are needed to confirm these findings.

Variability in the precise location of the transducers must also be considered. To minimize this problem, all surgeries were performed by the same individual. The presence of transducers and electrodes is a problem which is inherent to all sonometric studies. Additionally, it must be emphasized that findings in sheep are not necessarily applicable to humans. Although most dynamic valve studies have used an ovine model, species differences in tissue compliance and leaflet thickness might influence the results obtained.

*In conclusion*, studies of functional tricuspid regurgitation have been limited by the anatomic complexity of the normal tricuspid valve, the absence of simple methods to study right ventricular function, and a paucity of its clinical manifestations. In the present study, the tricuspid valve was shown to form a dynamic part of the right ventricle, and that its opening and closure is not simply a response to changes in pressure.

These data should have a significant impact on the evaluation and surgical treatment of functional tricuspid valve disease.

**Acknowledgements**

The authors thank Kathleen Billington, Holly Meskimen, and Leslie Trail for their support, which was essential to the completion of these experiments, and Jill Roberts for her editorial assistance.

**References**

1. Lansac E, Lim HS, Shomura Y, et al. A four-dimensional study of the aortic root dynamics. Eur J Cardiothorac Surg 2002;22:497-503
2. Goetz WA, Lim HS, Lansac E, Weber PA, Birnbaum DE, Duran CM. The aortomitral angle is suspended by the anterior mitral basal 'stay' chords. Thorac Cardiovasc Surg 2003;51:190-195
3. Goetz WA, Lim HS, Pekar F, et al. Anterior mitral leaflet mobility is limited by the basal stay chords. Circulation 2003;107:2969-2974
4. Hiro ME, Jouan J, Pagel MR, et al. Sonometric study of the normal tricuspid valve annulus in sheep. J Heart Valve Dis 2004;13:452-460
5. Gorman RC, McCaughan JS, Ratcliffe MB, et al. Pathogenesis of acute ischemic mitral regurgitation in three dimensions. J Thorac Cardiovasc Surg 1995;109:684-693
6. Pappas T. The Joy of Mathematics. 2nd edn. Wide World Publishing/Tetra, San Carlos, CA, USA, 1989:62
7. Fung YC. Biomechanics Motion, Flow, Stress, and Growth. Springer-Verlag, New York, NY, USA, 1990:358
8. Salgo IS, Gorman JH, III, Gorman RC, et al. Effect of annular shape on leaflet curvature in reducing mitral leaflet stress. Circulation 2002;106:711-717
9. Kreysig E. Advanced Engineering Mathematics. 8th edn. John Wiley & Sons, Inc., New York, NY, USA, 1999
10. Guyton AC. Textbook of Medical Physiology. 9th edn. WB Saunders, Philadelphia, PA, USA, 1996
11. McCarthy PM, Bhudia SK, Rajeswaran J, et al. Tricuspid valve repair: Durability and risk factors for failure. J Thorac Cardiovasc Surg 2004;127:674-685
12. Tsakiris AG, Mair DD, Seki S, Titus JL, Wood EH. Motion of the tricuspid valve annulus in anesthetized intact dogs. Circ Res 1975;36:43-48
13. Tei C, Pilgrim JP, Shah PM, Ormiston JA, Wong M. The tricuspid valve annulus: Study of size and motion in normal subjects and in patients with tricuspid regurgitation. Circulation 1982;66:665-671
14. Buckberg GD, Coghlan HC, Hoffman JI, Torrent-Guasp F. The structure and function of the helical heart and its buttress wrapping. VII. Critical importance of septum for right ventricular function. Semin Thorac Cardiovasc Surg 2001;13:402-416
15. Rademakers FE, Rogers WJ, Guier WH, et al. Relation of regional cross-fiber shortening to wall thickening in the intact heart. Three-dimensional strain analysis by NMR tagging. Circulation 1994;89:1174-1182
16. Rushmer RF, Crystal DK, Wagner C. The functional anatomy of ventricular contraction. Circ Res 1953;1:162-170
17. Torrent-Guasp FF, Whimster WF, Redmann K. A silicone rubber mould of the heart. Technol Health Care 1997;5:13-20
18. Greenbaum RA, Ho SY, Gibson DG, Becker AE, Anderson RH. Left ventricular fibre architecture in man. Br Heart J 1981;45:248-263
19. Lansac E, Lim KH, Shomura Y, et al. Dynamic balance of the aortomitral junction. J Thorac Cardiovasc Surg 2002;123:911-918
20. Hueb AC, Jatene FB, Moreira LF, Pomerantzeff PM, Kallas E, de Oliveira SA. Ventricular remodeling and mitral valve modifications in dilated cardiomyopathy: New insights from anatomic study. J Thorac Cardiovasc Surg 2002;124:1216-1224
21. Gorman JH, III, Gupta KB, Streicher JT, et al. Dynamic three-dimensional imaging of the mitral valve and left ventricle by rapid sonomicrometry array localization. J Thorac Cardiovasc Surg 1996;112:712-726
22. Tamiya K, Higashidate M, Kikkawa S. Real-time and simultaneous measurement of tricuspid orifice and tricuspid annulus areas in anesthetized dogs. Circ Res 1989;64:427-436
23. Coghlan C, Prieto G, Harrison TR. Movement of the heart during the period between the onset of ventricular excitation and the start of left ventricular ejection. Am Heart J 1961;62:65-82
24. Higashidate M, Tamiya K, Kurosawa H, Imai Y. Role of the septal leaflet in tricuspid valve closure. Consideration for treatment of complete atrioventricular canal. J Thorac Cardiovasc Surg 1992;104:1212-1217
25. Silver MD, Lam JH, Ranganathan N, Wigle ED. Morphology of the human tricuspid valve. Circulation 1971;43:333-348
26. Buchalter MB, Weiss JL, Rogers WJ, et al. Noninvasive quantification of left ventricular rotational deformation in normal humans using magnetic resonance imaging myocardial tagging. Circulation 1990;81:1236-1244
27. Hansen DE, Daughters GT, II, Alderman EL, Stinson EB, Baldwin JC, Miller DC. Effect of acute human cardiac allograft rejection on left ventricular systolic torsion and diastolic recoil measured by intramyocardial markers. Circulation 1987;76:998-1008